Sedimentary basins reconnaissance using the magnetic Tilt-Depth method

Article *in* Exploration Geophysics · August 2010

DOI: 10.1071/EG10007

CITATIONS
23

READS
1,353

6 authors, including:

Ahmed S. Salem

75 PUBLICATIONS **1,555** CITATIONS

SEE PROFILE

Simon Williams

Northwest University

136 PUBLICATIONS **2,761** CITATIONS

SEE PROFILE

Dhananjay Ravat

University of Kentucky

131 PUBLICATIONS **2,523** CITATIONS

SEE PROFILE

CSIRO PUBLISHING
www.publish.csiro.au/journals/eg *Exploration Geophysics*, 2010, **41**, 198–209

Sedimentary basins reconnaissance using the magnetic Tilt-Depth method

Ahmed Salem[1,2,5] Simon Williams[1,2] Esuene Samson[2] Derek Fairhead[1,2]
Dhananjay Ravat[3] Richard J. Blakely[4]

[1]GETECH, Kitson House, Elmete Hall, Elmete Lane, Leeds, LS8 2LJ, UK.
[2]School of Earth and Environment, University of Leeds, Leeds, LS2 9JT, UK.
[3]Earth and Environmental Sciences, University of Kentucky, 101 Slone Building, Lexington, KY 40506, USA.
[4]U.S. Geological Survey, 345 Middlefield Road, Menlo Park, CA 94025, USA.
[5]Corresponding author. Email: Ahmed.Salem@getech.com

Abstract. We compute the depth to the top of magnetic basement using the Tilt-Depth method from the best available magnetic anomaly grids covering the continental USA and Australia. For the USA, the Tilt-Depth estimates were compared with sediment thicknesses based on drilling data and show a correlation of 0.86 between the datasets. If random data were used then the correlation value goes to virtually zero. There is little to no lateral offset of the depth of basinal features although there is a tendency for the Tilt-Depth results to be slightly shallower than the drill depths. We also applied the Tilt-Depth method to a local-scale, relatively high-resolution aeromagnetic survey over the Olympic Peninsula of Washington State. The Tilt-Depth method successfully identified a variety of important tectonic elements known from geological mapping. Of particular interest, the Tilt-Depth method illuminated deep (3 km) contacts within the non-magnetic sedimentary core of the Olympic Mountains, where magnetic anomalies are subdued and low in amplitude. For Australia, the Tilt-Depth estimates also give a good correlation with known areas of shallow basement and sedimentary basins. Our estimates of basement depth are not restricted to regional analysis but work equally well at the micro scale (basin scale) with depth estimates agreeing well with drill hole and seismic data. We focus on the eastern Officer Basin as an example of basin scale studies and find a good level of agreement between previously-derived basin models. However, our study potentially reveals depocentres not previously mapped due to the sparse distribution of well data. This example thus shows the potential additional advantage of the method in geological interpretation. The success of this study suggests that the Tilt-Depth method is useful in estimating the depth to crystalline basement when appropriate quality aeromagnetic anomaly data are used (i.e. line spacing on the order of or less than the expected depth to basement). The method is especially valuable as a reconnaissance tool in regions where drillhole or seismic information are either scarce, lacking, or ambiguous.

Key words: Australia, basement, USA.

Introduction

The past decade has seen a wealth of new interpretation methods and refinements to existing geophysical methods to map subsurface geological structures from aeromagnetic data. With more sophisticated acquisition systems and GPS navigation, the resolution of total magnetic field data and their gradients have improved dramatically. This improvement in data resolution has allowed the application of more powerful computational methods to interpret these surveys often using higher (2nd and 3rd) order derivatives (Nabighian et al., 2005).

The Euler deconvolution method has proved a popular interpretation method which has evolved in significant theoretical ways following the original two-dimensional (2D) (profile) work of Thompson (1982) and the three-dimensional (3D) (grid) implementation by Reid et al., 1990. For example, Mushayandebvu et al. (2001) introduced 'extended Euler' containing a second equation, known as a rotational constraint, that can be applied to profile and gridded data in order to generate dip and susceptibility-contrast estimates based on the assumption of a contact or dyke model (Mushayandebvu et al., 2004; Williams et al., 2005).

An alternative approach is described here: known as Tilt-Depth (Salem et al., 2007), this method estimates depth directly from first-order derivatives of the observed magnetic field, similar to the local wavenumber methodology (e.g. Thurston and Smith, 1997), which uses third-order derivatives. These methods have a distinct advantage over the more commonly used Euler deconvolution method in that they produce depth estimates that relate directly to individual sections of anomalies, whereas the Euler solutions are generated from a series of overlapping windows that results in multiple solutions of varying quality. In addition, the Euler method requires the selection of an appropriate window size and structural index. Each Euler window location will generate a source depth solution and thus over a single anomaly a multiple set of solutions will be generated, resulting in the need to distinguish between reliable/robust solutions and weakly constrained solutions. The scatter of solutions arises from non-idealised, multiple and/or partial source geometries within a given window (Ravat, 1996). This scatter of solutions does not occur in the Tilt-Depth method thus making it easier to undertake post solution analysis and mapping of the data. The structural geometry of the source in the Tilt-Depth method is, however, implicitly fixed by assuming the vertical contact model, whereas Euler can assume an appropriate structural index value to match the geological structures being investigated.

 10.1071/EG10007 0812-3985/10/030198

In this paper, we show the results of the Tilt-Depth method (Salem et al., 2007) applied to continental-scale magnetic datasets for onshore USA and Australia to map the basement. The method also works well at a local scale with an example from Olympic Peninsula, USA to map tectonic elements of the region and the Eastern Officer Basin, Australia to map basin architecture. The Tilt-Depth method is based on simple theory, that relies only on first-order derivatives, and thus is less susceptible to noise than other methods such as Source Parameter Imaging (SPI) (Thurston and Smith, 1997) and the combined analytic signal-Euler method (AN-EUL) (Salem and Ravat, 2003), which require higher order derivatives. Since Tilt-Depth estimates are anomaly specific, they can identify anomaly interference caused by geological complexities, allowing for solutions to be either accepted or rejected. The physical model used in the Tilt-Depth method is a buried vertical 2D contact. This is an ideal first approximation for mapping subsurface structures and has been successfully used to determine magnetic depth for over 50 years (e.g. Vacquier et al., 1951). Since sub-surface structures can be complex in nature, the 2D contact model used to generate and map the physical parameters of the geology is at best an approximation and needs further refinement and support from additional depth inversion methods and/or using additional geophysical and geological datasets.

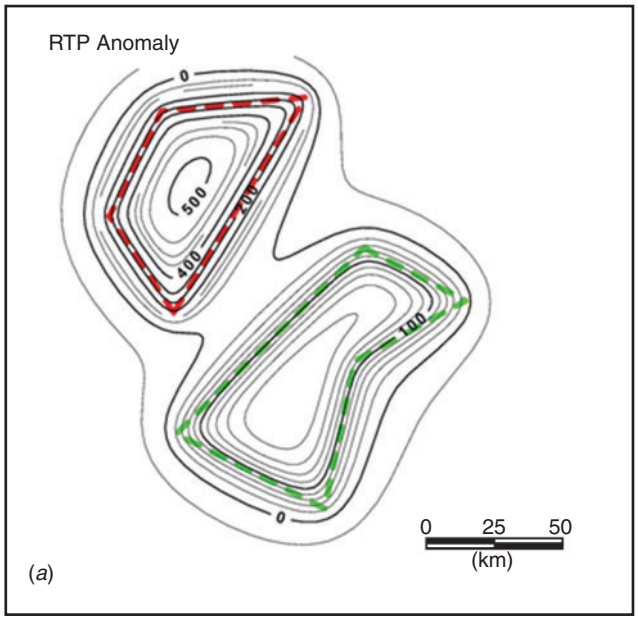

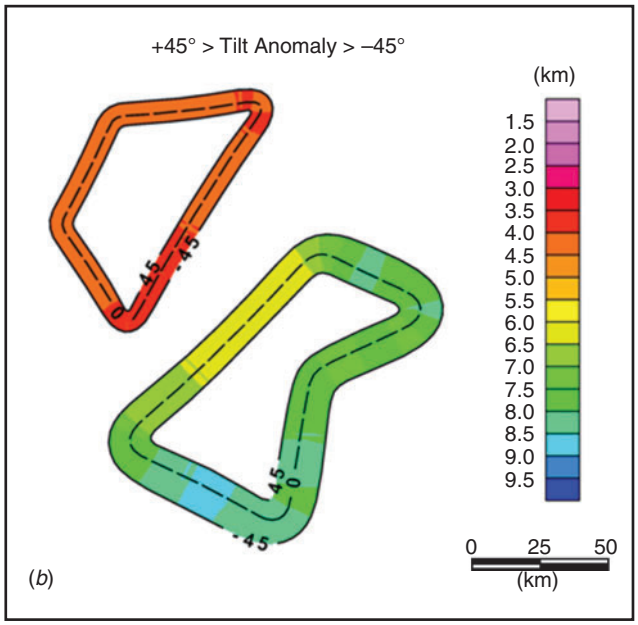

Fig. 1. (*a*) The contoured reduced to the pole (RTP) field over the 3D model structures (outlined as colour polygons) at 4 km depth (NW body) with susceptibility 0.002 SI and at 8 km depth (SE body) with susceptibility 0.001 SI. (*b*) The Tilt anomaly restricted to values lying between ±45°. The colour fill represents the estimated depth, which varies in this case due to anomaly interference and non-2D structural affects etc.

Background of the Tilt-Depth method

The tilt angle is the generalised definition for the local phase (Miller and Singh, 1994) and was re-introduced by Verduzco et al. (2004) and is defined as:

$$\theta = \tan^{-1}\left(\frac{\frac{\delta M}{\delta z}}{\frac{\delta M}{\delta h}}\right), \qquad (1)$$

where $\delta M/\delta h = \sqrt{(\delta M/\delta x)^2 + (\delta M/\delta y)^2}$, and $\delta M/\delta x$, $\delta M/\delta y$ & $\delta M/\delta z$ are first-order derivatives of the magnetic field M in the x, y, and z directions. Since the tilt angle consists of the ratio of the vertical and horizontal derivatives, the resulting tilt angle function contains no information on either the strength of the geomagnetic field M or the susceptibility of the causative bodies, thus by implication contains no information on the magnetization of the sub-surface bodies. It does, however, contain information on the depth of the source of the anomaly and the geomagnetic field inclination and declination. The 'arctan' function also limits the magnitude of the tilt angle to ±90° (or $\pm\pi/2$) and is similar to the automatic gain control filter used in processing of potential field data (Rajagopalan and Milligan, 1994) as in traditional seismic-reflection processing, permitting low-amplitude anomalies to be seen as clearly as high amplitude anomalies. If the magnetic field is appropriately reduced to the pole (RTP), then the geomagnetic inclination and declination dependency of the induced anomaly is removed, thus positioning the zero

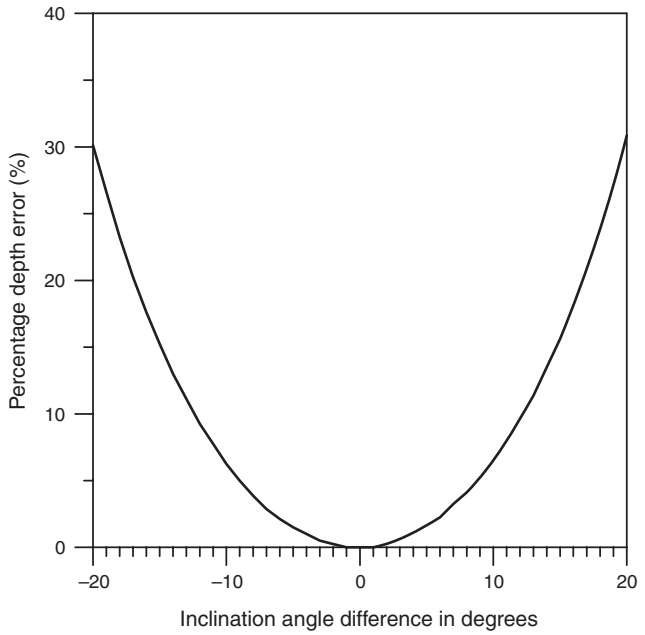

Fig. 2. Depth errors as a percentage of the actual depth with varying differences in inclination angle between the induced and remanent magnetization fields.

contour of θ close to the boundary of the causative body. The Tilt-Depth method uses the RTP field and derives the relationship between the tilt angle, horizontal location and depth of a simple buried vertical 2D contact model as

$$\theta = \tan^{-1}\left(\frac{h}{z_c}\right), \qquad (2)$$

where h is the horizontal location of the contact and depth z_c is the depth. Equation 2 indicates that the location of the contact ($h = 0$) corresponds to the zero tilt angle and the depth corresponds to the horizontal distance between tilt angles of 0° and ±45° (i.e. corresponding to $h = \pm z_c$). Other tilt angles can be used; e.g. 26.6° where $h = 0.5\ z_c$, etc. Thus depth estimates can be derived directly from the tilt angle map by simply measuring the distance between appropriate contours, hence the name Tilt-Depth. We further define a quantity D_N, the perpendicular distance between contours $\theta = -N$ and $\theta = +N$, where N is in degrees. D_N is directly related to source depth.

We use a colour-contour fill method to display our results, as illustrated in Figure 1, compared to the grey fill method used in Salem et al. (2007) to enhance the image and allows for rapid visual inspection of depth variations. In Figures 1*b*, 3*b*, 4*c*, 5*b*

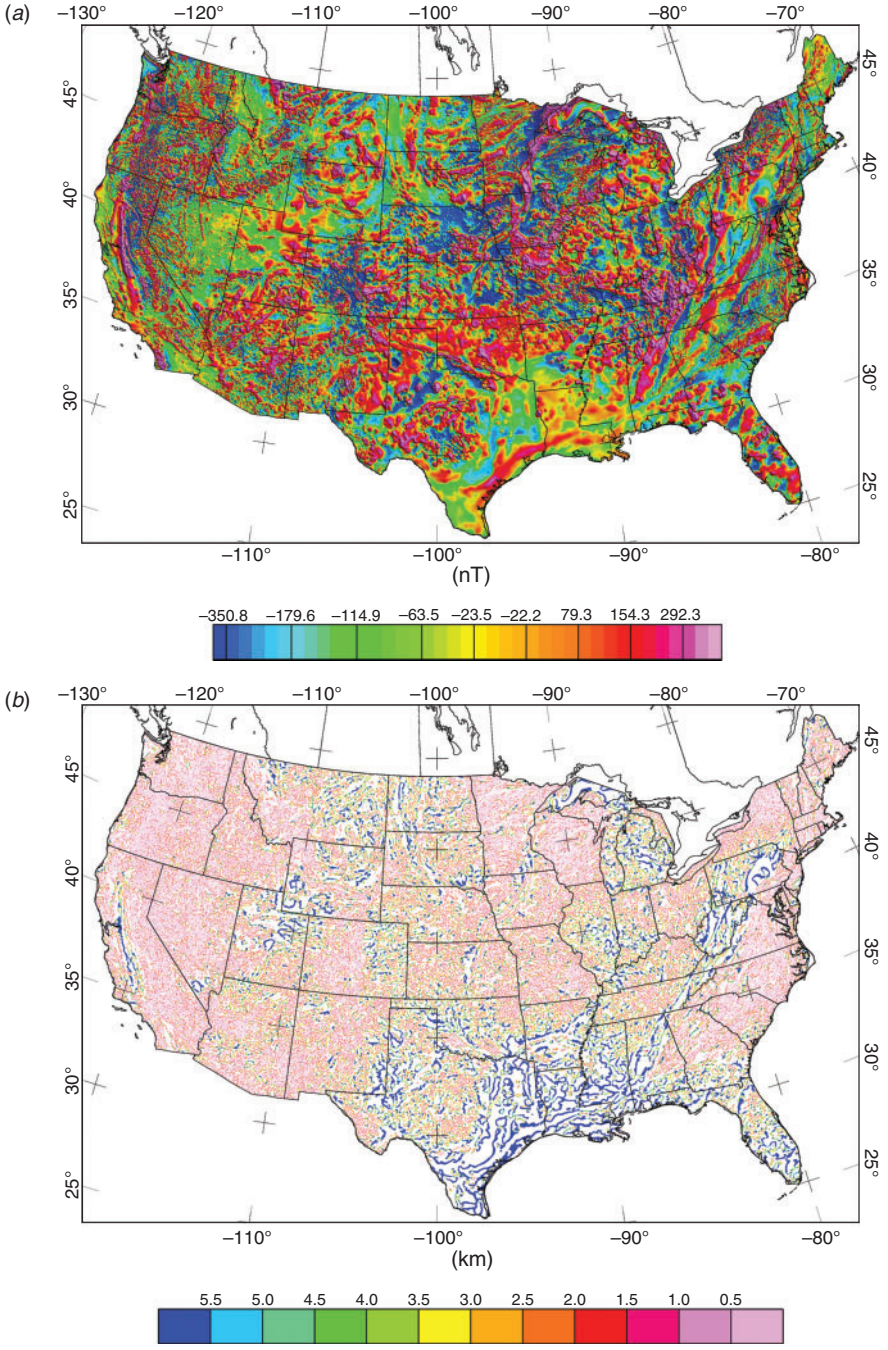

Fig. 3. (*a*) Magnetic map of the USA (North American Magnetic Anomaly Group, 2002), reduced to the pole using the method of Swain (2000). (*b*) The Tilt-Depth colour map of the USA. (*c*) 1° average sedimentary thickness map of the USA (Laske and Masters 1997). (*d*) Tilt-Depth contour map after regridding at 0.25° spacing (Figure 1*b*). (*e*) Regression analysis plot of the grid node depths of Figure 3*c* and 3*d*. Red line shows the best fit of linear regression. (*f*) Difference between the sedimentary thickness map and the Tilt-Depth estimates.

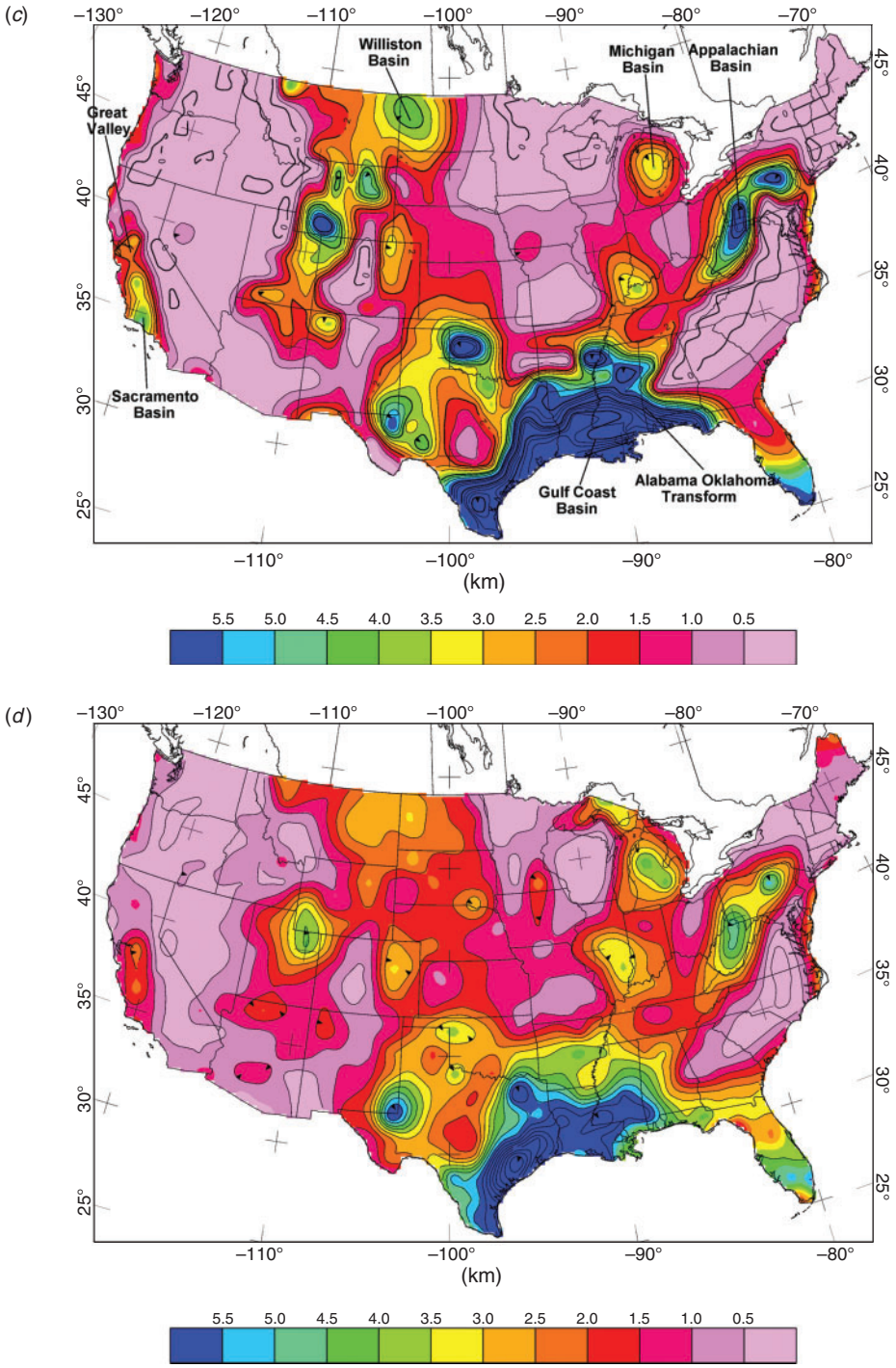

Fig. 3. (*continued*)

and 6*a* we have simplified the Tilt angle maps that range in amplitude from ±90° to just plotting the zero and the +45° and –45°, thus allowing the greatest impact of the colour over a continental scale image. In Figure 1*b*, the assigned colour is based of the perpendicular distance D_{45} between the ±45° contours. Thus colour is a direct indication of depth to source, warm colours indicating shallow sources and cool colours indicating deep sources. This display method also allows the interpreter to qualitatively distinguish between reliable and unreliable solutions in locations of anomaly interference. Figure 1*b* illustrates $45° > \theta > -45°$ resulting from two closely spaced structures outlined in Figure 1*a*. The shallow (4 km) NW body has a higher frequency anomaly, which interferes with the longer wavelength anomaly from the deeper (8 km) source resulting in a shallower estimate (≈6 km) for that part of the long wavelength anomaly located closest to the NW body.

Error analysis

Depths derived from D_N are prone to errors due to deviations from the underlying model assumptions: e.g. contacts or faults that are not 2D, gradational susceptibility contrasts, the presence of remanent magnetization, non-vertical contacts, and nearby magnetic structures that interfere with the target anomaly. To test the effect of remanent magnetization, we generated magnetic data for a contact at a depth of 4 km with vertical induced

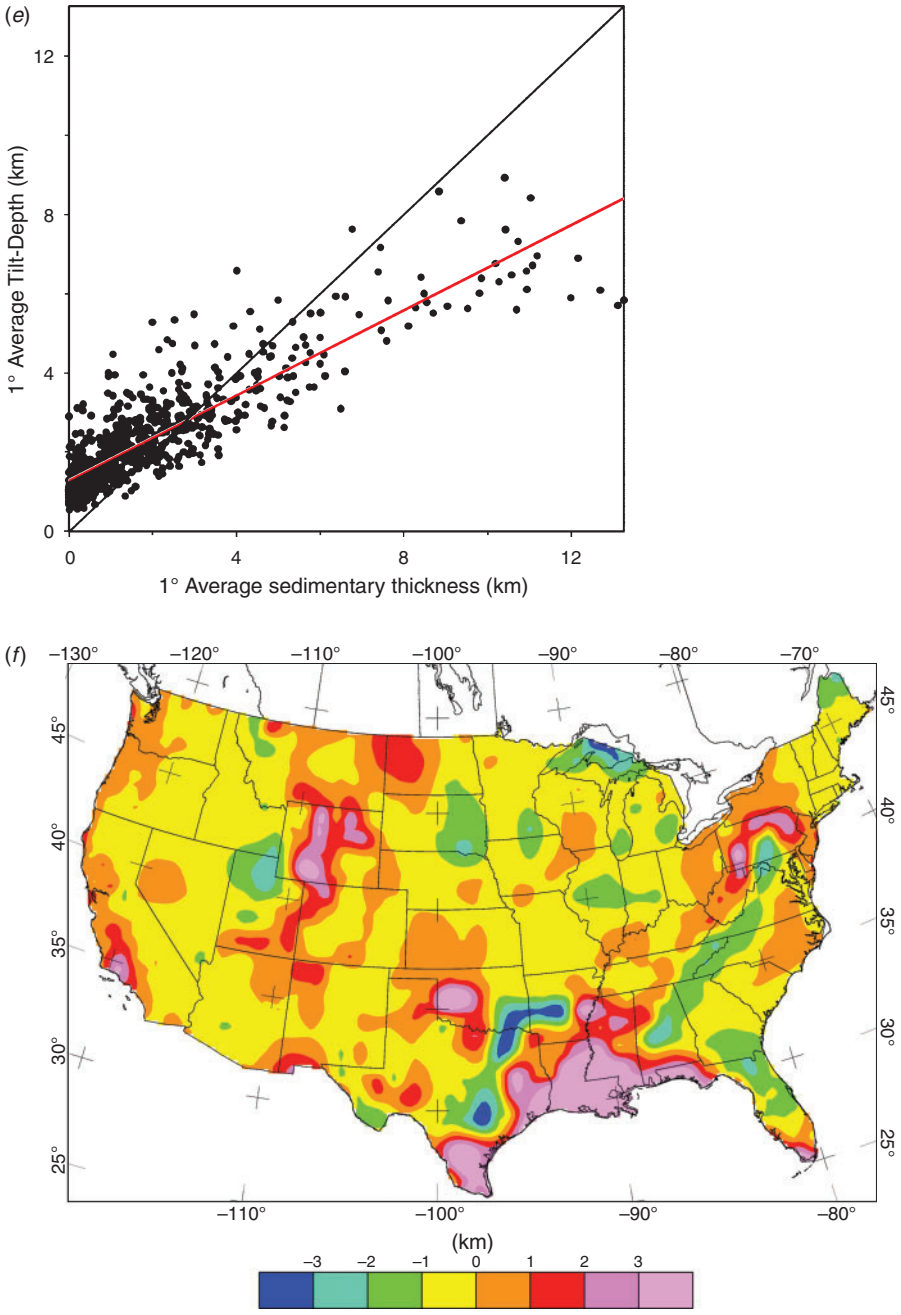

Fig. 3. (*continued*)

magnetization. We then added to this induced field a remanent magnetization field with the strength equal to the induced field but with inclination angles that varied from –20° to 20° with respect to the induced vertical inclination angle. As expected, the introduction of remanent magnetization does affect the results. The depth estimates are overestimated by up to 30% of the actual depth (Figure 2).

Applications

The depth method requires a well constrained RTP field. The orientation of the Earth's magnetic field varies considerably across large continental areas such as USA and Australia. For this reason, calculation of the reduced-to-pole magnetic field using a single inclination and declination over a large region is unsatisfactory. Swain (2000) presents a method for calculating a continuous reduction to the pole taking into account the varying inclination and declination across large study areas. We have successfully applied this algorithm to a 1 km grid of the Total Magnetic Intensity databases of USA and Australia. We also applied the method to the local-scale, relatively high-resolution aeromagnetic survey over the Olympic Peninsula of Washington State.

1. Regional Data of the Continental USA

Figure 3*a* shows the RTP magnetic anomalies of the onshore part of the USA, derived from the magnetic anomaly grid of North America (North American Magnetic Anomaly Group, 2002). Although the grid cell size is 1 km, many areas have flight line spacing as large as 5 to 10 km. Figure 3*b* shows our Tilt-Depth analysis applied to continental USA magnetic anomalies. This map was calculated in five steps: (1) upward continuing the anomalies by 1 km, (2) reducing the anomalies to the pole,

(3) calculating and displaying the Tilt derivative in terms of the zero contour and the pairs of contours used to estimate depth, (4) applying a second algorithm to map D_{25}, the distance between the ±25° (where $D_{25} = 0.4663\ z_c$) tilt derivative contours, and (5) subtracting the observation altitude and the upward continuation distance (1.305 km). The map indicates extensive areas of shallow magnetic basement (depth <1 km), punctuated by numerous deeper areas corresponding to known sedimentary basins (see Bally, 1989). The greatest depths are observed in the region north of the Gulf Coast Basin extending inland to the location of the NW–SE Alabama–Oklahoma Transform (Thomas, 1991), where 'estimated' depths exceed 6 km. Tilt-Depths (Figure 3*b*) retain a texture similar to that of a magnetic derivative map, so that the Appalachian Basin is represented by bands with a strong NE–SW structural trend, the colour providing additional information on the basement depth. Figure 3*b* shows a narrow band of deep magnetic sources along the length of the Great Valley in California. This probably results from the high-amplitude, long-wavelength Great Valley anomaly, believed to be caused by Jurassic-age ophiolites that underly the Great Valley and neighbouring Coast Ranges. The ophiolites lie at shallow depth along the north-east side of the anomaly but extends to >15 km depth along the south-eastern side of the anomaly (Jachens et al., 1995) (see Figure 3*c* for locations of features). By contrast, strong linear trends are far less apparent within Paleozoic cratonic basins (e.g. Michigan Basin, Illinois Basin, Williston Basin).

For a regional assessment of the depths to magnetic basement, we use a global 1° average sedimentary thickness map (Figure 3*c*) compiled by Laske and Masters (1997). This map was prepared by hand-digitising and/or averaging (as appropriate) data from the oceans and digitising the tectonic map of the world by Exxon production research group for continental areas (including shelves).

The spatial resolution of the Tilt-Depth estimates shown in Figure 3*b* is dependent on the resolution of the original magnetic grids from which they are derived, which is 5–10 km for two-thirds of the central states and does not reflect the 1 km grid spacing of the NAMAG (2002) database. Nonetheless, to allow direct comparison with the 1° average sedimentary thickness map, the Tilt-Depths shown in Figure 3*b* were assigned to point values along the zero tilt contour and then these points were interpolated to a 0.25° grid using minimum curvature to maximise the spatial resolution of Tilt-Depth results (Figure 3*d*).

At this resolution, Tilt-Depth shows a striking visual correlation with the 'ground-truthing' provided by the 1° average sedimentary thickness map. Figure 3*e* shows a cross-plot of grid nodes from the low-pass filtered Tilt-Depth (at 0.25° spacing) and sedimentary thickness resampled at the corresponding locations. The cross-plot shows a clear linear

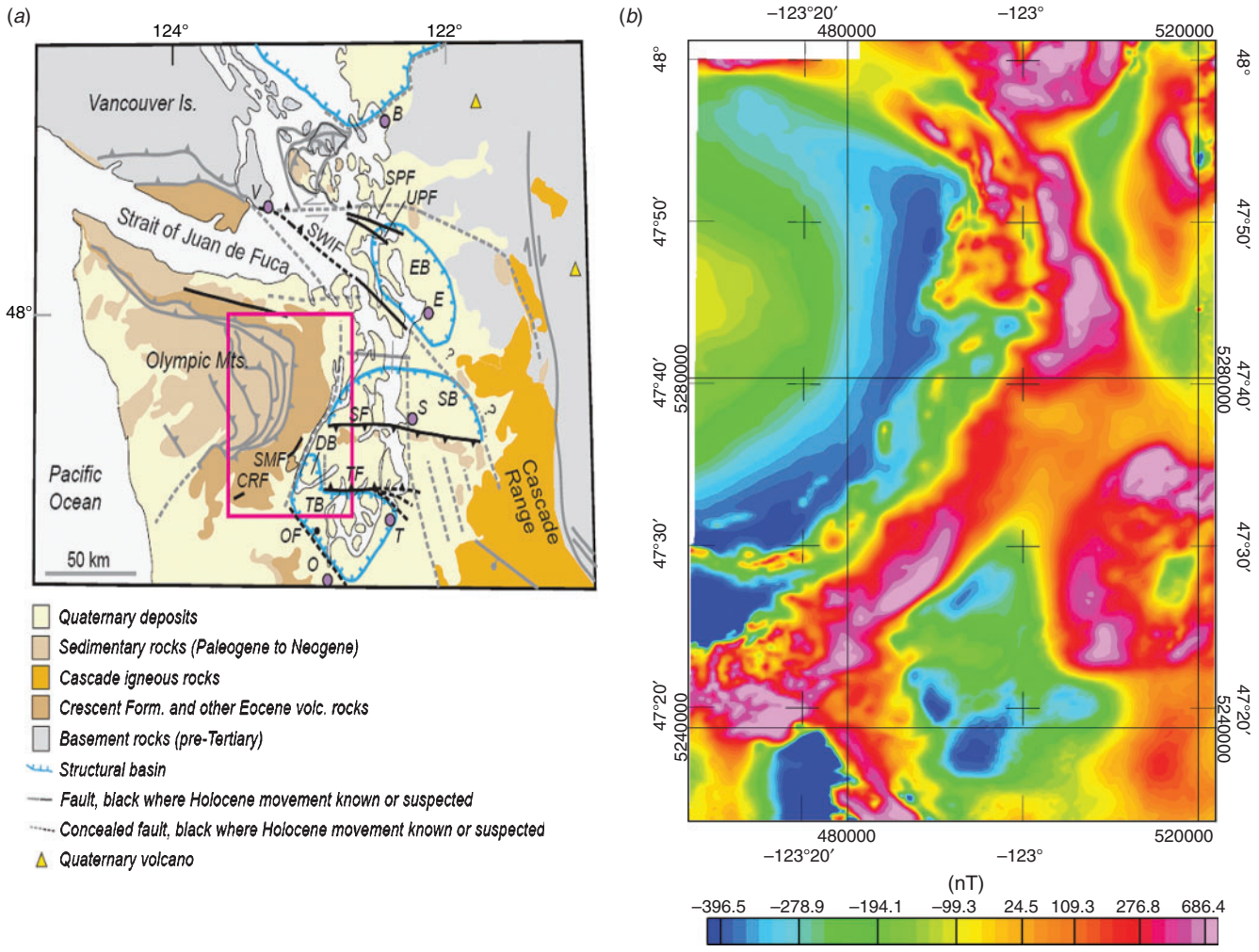

Fig. 4. (*a*) Geological map of the Olympic Peninsula and surrounding region. Red rectangle shows area of Figure 4*b* and 4*c*. S, Seattle; B, Bellingham; T, Tacoma; V, Victoria; O, Olympia; E, Everett. (*b*) Aeromagnetic map (RTP) of the Olympic Peninsula (Blakely et al., 1999). (*c*) Application of the Tilt-Depth methodology to magnetic anomalies of the Olympic Peninsula. Labels refer to features discussed in text.

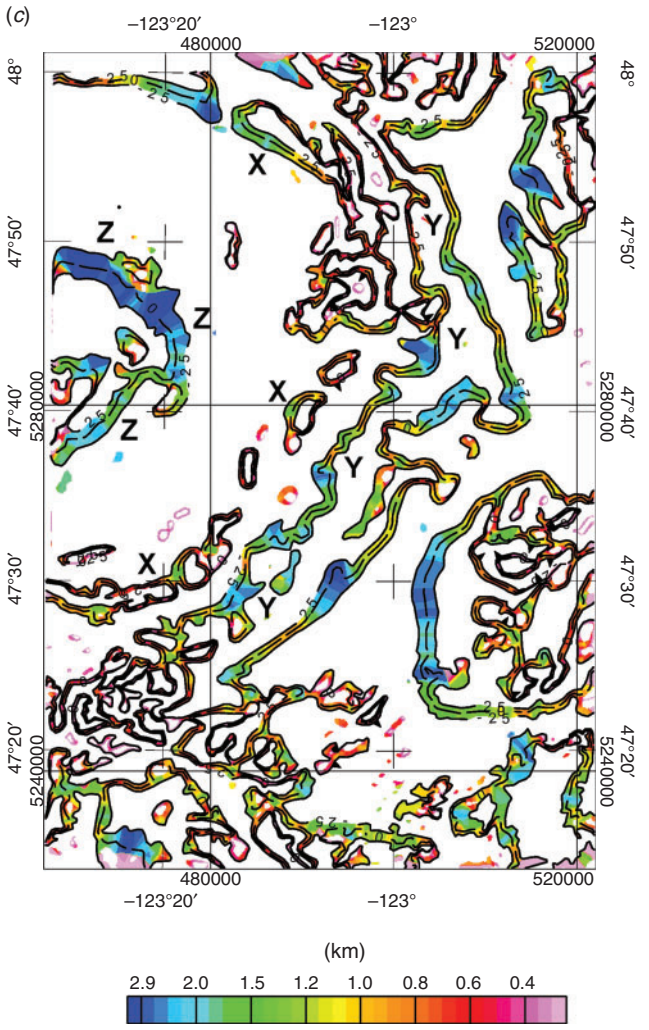

Fig. 4. (*continued*)

relationship between the Tilt-Depth values and sediment thickness. The correlation coefficient, which shows the degree of similarity between the two datasets, is 0.86 with features on these maps are not significantly shifted in their location. While the scatter plot in Figure 3*e* shows that the individual point correlation may lie within ±2 km, the difference map (Figure 3*f*) has large values only in a few locations – especially where sedimentary package thicknesses are large. These areas are correlated with areas of flight line spacing greater than 4 km suggesting that those magnetic anomalies may be aliased, and not well determined, when over regions of shallow basement, and hence artificially yielding smoother features and deeper Tilt-Depths. It is not clear that in all these large difference regions the Laske and Masters data (or the original databases) are well constrained, but where there is drillhole information the Laske and Masters 1° map appears to be accurate. There could be many causes of large differences between the sedimentary thickness database and the Tilt-Depth estimates. There are regions where drillholes encountering crystalline basement may not be present or sparse. Tilt-Depth may produce incorrect deep estimates where the aeromagnetic coverage may not be optimum (too sparse) for the depth of the crystalline basement encountered in the region. And lastly, the assumptions of the Tilt-Depth may not be entirely satisfied in a particular situation. In an overall sense, however, the examination of spatial differences (Figure 3*f*) suggests that where depth to basement based on the Exxon map is greater than 4 km, the Tilt-Depth estimates tend to underestimate the true basin depth. Systematic underestimation of source depths implies an incorrect assumption of source geometry (the greater the depth to the top of a source, the more the source must fit the exact geometric assumption of the magnetic contact), a problem well known from other magnetic depth estimation methods and can be corrected *a posteriori* using regional correction factors.

We have also critically examined a portion of this map by examining it against the drillholes penetrating Precambrian basement in a few of the contiguous states in the eastern USA (Kentucky, Ohio, West Virginia, Pennsylvania and New York). We found that the Laske and Masters' 1° data agreed with the total sedimentary package thickness from the drillholes within a couple hundred metres. Several Appalachian regions do not have drillholes penetrating crystalline basement. State geological surveys have in their databases estimated depths to Precambrian basement based on the deepest formation encountered in the drillholes or from seismic surveys. We found that in these 'estimated basement depths' diverged significantly from the Laske and Masters (1997) map; however, the tilt-depth estimates agreed more closely with the Laske and Masters database, validating their interpolation through these areas.

2. Higher resolution data of Olympic Peninsula, Washington, USA

Distinctive magnetic anomalies of the Olympic Peninsula, Washington, provide a useful application of the Tilt-Depth method in investigation of detailed geological or tectonic elements of a region. The Olympic Peninsula lies within the forearc of the Cascadia subduction zone, where the Juan de Fuca plate is subducting at low angle beneath North America (Wells et al., 1998). The Olympic Mountains represent an east-plunging anticline consisting of two distinct terranes: an essentially non-magnetic core of highly deformed Tertiary sedimentary rocks that underlie the Olympic Mountains and a periphery of early Eocene basalt and marine sediments that wrap around the eastern margin of the Olympic Mountains (Tabor and Cady, 1978; Figure 4*a*). The periphery rocks consist primarily of early to middle Eocene Crescent Formation basalts and associated volcanic and sedimentary rocks, an over-thickened volcanic assemblage of oceanic affinity (e.g. Snavely and Wagner, 1963). The Crescent Formation in this locale has both an upper and lower member (Tabor and Cady, 1978). Magnetic anomaly analysis and susceptibility measurements show that the upper member is highly magnetic, typical of basaltic terranes, whereas the lower member is only weakly magnetic, possibly due to local metamorphism to green schist facies (Blakely et al., 2009).

Magnetic anomalies in Figure 4*b* are based on an aeromagnetic survey flown in 1997 by the USA Geological Survey (Blakely et al., 1999). Flight altitude was nominally 300 m over flat to moderate terrain, but significantly higher altitudes were necessary over river valleys and along the eastern margin of the Olympic Mountains. Most of the study area was flown along north–south flight lines spaced 400 m apart and along east–west tie lines spaced 8 km apart.

Figure 4*c* shows an application of the Tilt-Depth methodology to the Olympic Peninsula, where a variety of important geological contacts were identified. The boundary between highly magnetic upper member and weakly magnetic lower member Crescent Formation (Figure 4*c*, label Y) was identified by the Tilt-Depth method as a fundamental magnetic contact in the study area. This is not surprising, considering the obvious magnetic anomaly gradients associated with this contact (Blakely et al., 2009). However, the steeply dipping thrust contact between non-

magnetic sedimentary core rocks and weakly magnetic lower member Crescent Formation (Figure 4*c*, label X), more difficult to discern in the magnetic anomaly map (Figure 4*b*), was identified by the Tilt-Depth method as a discontinuous contact. Of particular interest, the Tilt-Depth method located a deep magnetic source (3 km) beneath non-magnetic core sedimentary rocks (Figure 4*c*, label Z). The magnetic anomalies associated with this magnetic source are very subdued (Figure 4*b*), indicating the power of the Tilt-Depth method to discern sources that cause only subtle magnetic anomalies.

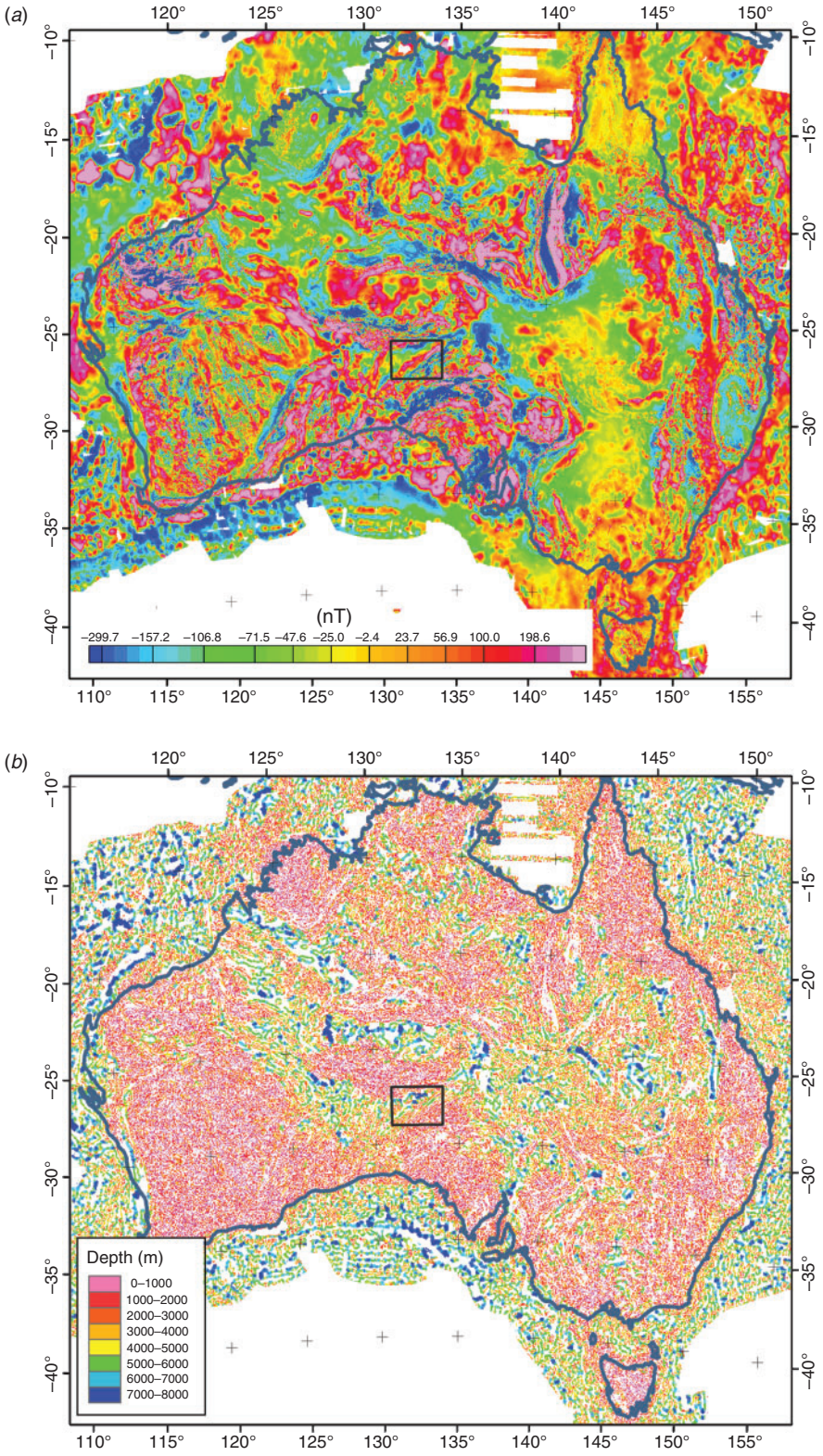

Fig. 5. (*a*) Magnetic map of Australia (Milligan et al., 2004), reduced to the pole using the method of Swain (2000). (*b*) The Tilt-Depth colour map of Australia. (*c*) Sedimentary thickness map of Australia derived from geological, seismic and well data (Borissova and Kilgour, 2000). (*d*) Tilt-Depth contour map derived by interpolating and low-pass filtering the results in the original Tilt-Depth map (Figure 5*b*).

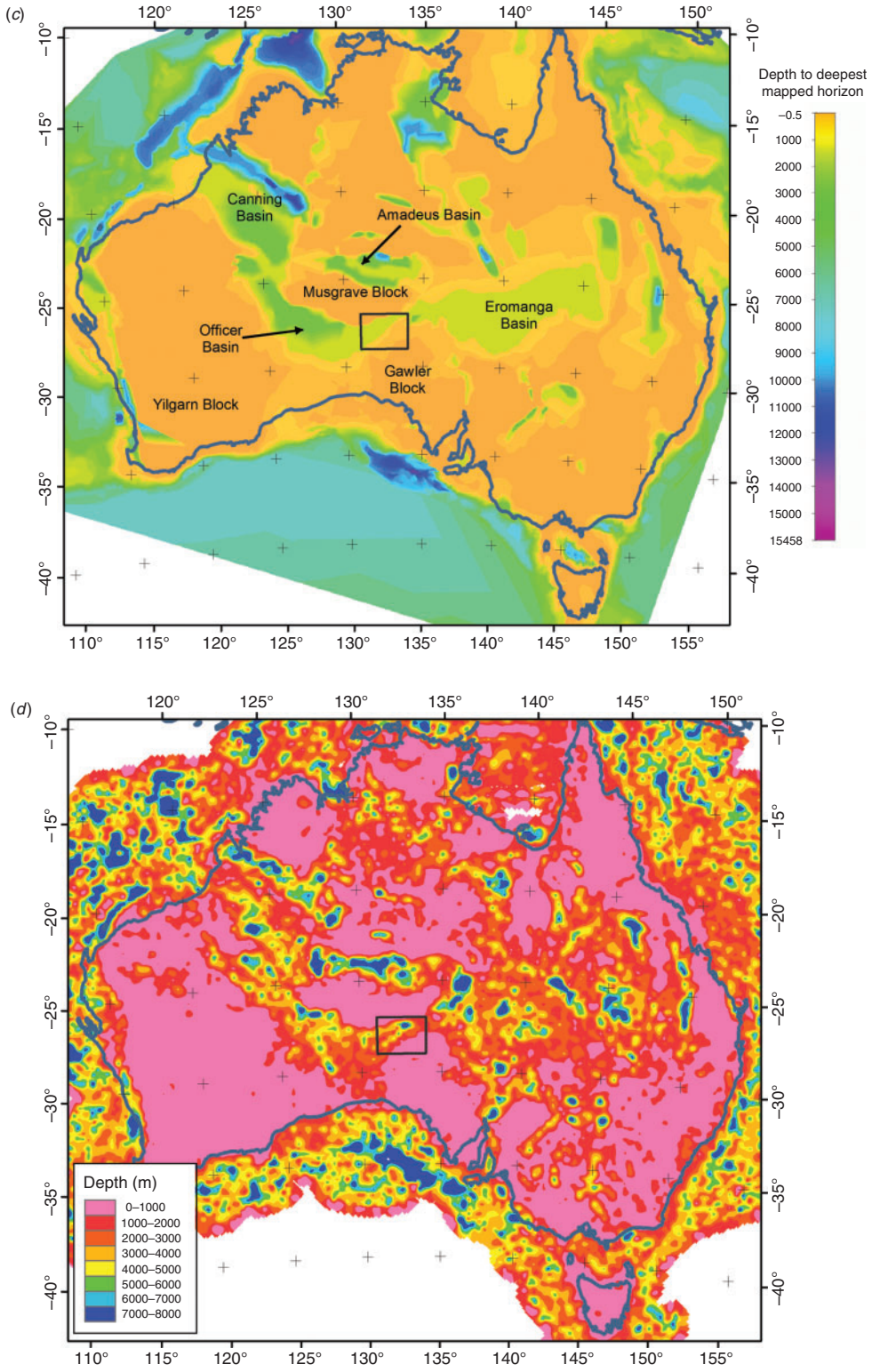

Fig. 5. (*continued*)

3. Australia

Australia is an excellent continental area to demonstrate the method, since there is a new reprocessed aeromagnetic database (Milligan et al., 2004). The aeromagnetic database of Australia was compiled from a large number of aeromagnetic surveys of varying flight line spacing. The Australian Geomagnetic Reference Field (AGRF) has been removed and the final data are presented with a cell size of 0.01 degree (≈1 km). The Tilt-Depth method has been applied to a reduced-to-pole magnetic anomaly map for all Australia (Figure 5*a*) following the same five-step methodology described for the USA. Figure 5*b* shows the results of the Tilt-Depth method. Qualitatively, the results show a good correlation with the known areas of shallow basement and sedimentary basins. Areas of exposed basement such as the Yilgarn, Musgrave, and Gawler Blocks correspond to Tilt-Depth values consistently less than 1 km, while estimated depths within the Amadeus, Officer and Canning Basins exceed 8 km. For a more quantitative comparison, Figure 5*c* shows a

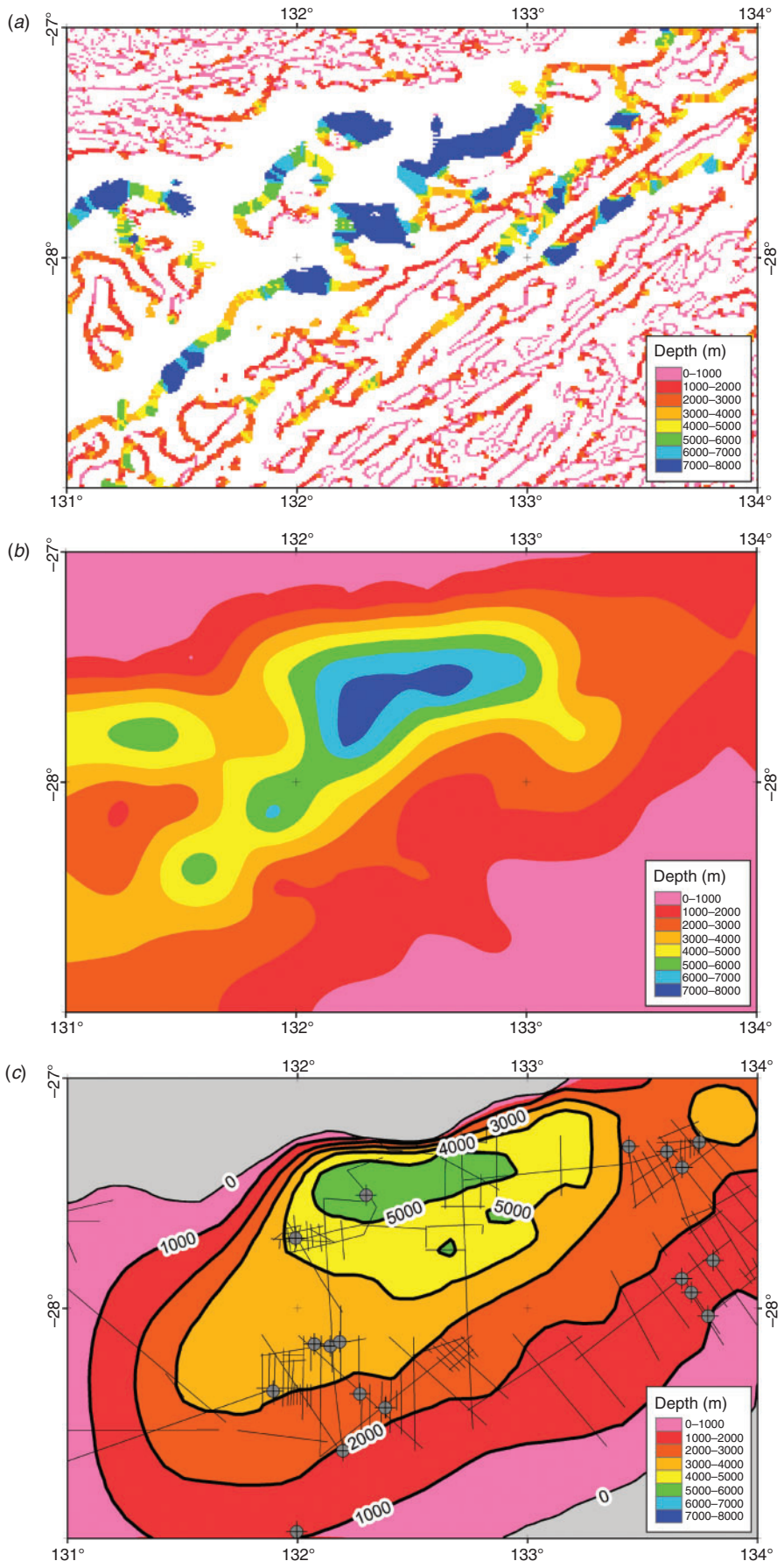

Fig. 6. (*a*) Tilt-Depth results for the Eastern Officer Basin. (*b*) Tilt-Depth contour map for the Eastern Officer Basin. (*c*) Sediment thickness contours for the Eastern Officer Basin, redrawn from Haddad et al., 2001. The contours were generated using data from wells (locations shown by circular symbols) and depth converted seismic lines (black lines).

section of the public domain depth to basement map for Australia, available from Geoscience Australia (Borissova and Kilgour, 2000). This grid was derived from contour maps derived from seismic reflection interpretation, refraction, well and geological information (Heine, 2007, and references therein). The basement depth map is freely available as an image (shown in Figure 5*c*), although information about the data coverage and method of interpolation is not provided. We have interpolated the Tilt-Depth values in Figure 5*b* by minimum curvature to a 5 km grid with a 30 km low-pass filter applied (Figure 5*d*). Visual comparison shows good agreement between the two maps, particularly onshore where both datasets are likely to be better constrained. The filtered Tilt-Depth results in Figure 5*d* contain shorter wavelength variations than the Geoscience Australia map. The amount of filtering used to derive Figure 5*d* is somewhat arbitrary, and a longer wavelength filter would produce a smoother grid similar to Figure 5*c*. The following example investigates the extent to which the shorter wavelength variations within Figure 5*d* are robust.

Figure 6*a* shows an example of the Tilt-Depth results for a small subset of the results for Australia. The Eastern Officer Basin area was chosen so that we could compare our estimates of basement depth to the independently derived sediment thickness map presented by Haddad et al., 2001. The boxes in each panel of Figure 5 show the outline of their detailed study area. Haddad et al. (2001) estimated sediment thickness based on a combination of well log and depth-converted seismic data. These irregular data were then gridded using a minimum curvature algorithm to produce the sediment thickness contours. The Tilt-Depth estimates for this area are shown in Figure 6*a*. Figure 6*b* presents the result of gridding the Tilt-Depth estimates by minimum curvature onto a 2 km grid with a 30 km low-pass filter. We have digitised the sediment thickness contours from Haddad et al. (2001) and interpolated these contours to a grid so that the values can be displayed using the same colour scale as the Tilt-Depth results. The basement depth estimated from the magnetic data correlates well with the sediment thickness contours (Figure 6*c*) where these contours are constrained by drilling. The maximum sediment thickness in the Tilt-Depth results is 1 to 2 km greater than, and lies slightly to the south of, the thickest sediments determined from the available drilling and seismic data (Haddad et al., 2001). The Tilt-Depth map also suggests additional, minor depocentres to the west of the area.

Discussion and conclusion

We have applied the Tilt-Depth method to two continental magnetic datasets covering the onshore USA and Australia. For each continent, we have constructed basement depth maps based on the Tilt-Depth method. We find a good correlation with known areas of shallow basement and sedimentary basins. In the USA, to quantitatively evaluate the results, we low-pass filtered the calculated depths, and regridded to a 1/4 degree sample interval, in order to compare with a resampled 1/4 degree grid of sediment thicknesses based on drilling data (Laske and Masters, 1997). The resulting depth maps for the two datasets show good correlation between basement highs and lows. Quantitatively, the overall correlation coefficient between the two datasets was 0.86, indicating that there is very little lateral offset in the depth features of the two maps. We also applied the Tilt-Depth method to a local-scale, relatively high-resolution aeromagnetic survey over the Olympic Peninsula of Washington State. The Tilt-Depth method successfully identified a variety of important tectonic elements known from geological mapping. Of particular interest, the Tilt-Depth method illuminated deep (3 km) contacts within the non-magnetic sedimentary core of the Olympic Mountains, where magnetic anomalies are subdued and low in amplitude. In Australia, we have compared our estimates of basement depth to a map of sediment thickness derived independently from well and seismic data in the eastern Officer Basin, and found a good level of agreement between these independently-derived basin models.

Generally, a 2D buried vertical contact is shown to be a robust model suitable for rapidly evaluating the depth and structure of magnetic basement. Our tests indicate that results are affected by uncertainties in geomagnetic inclination, but, if induced magnetization is dominant, inclination uncertainties are typically less than a few degrees. When applying reduction to the pole over large continental areas, it is important to use RTP methods that allow for spatially varying geomagnetic field declination and inclination (Swain, 2000). The presence of remanence will affect our results. The importance of remanent magnetization can often be established from the geological setting or identified at the RTP stage of data processing. Thus the Tilt-Depth method is applicable to a wide range of geological structures. As with any inverse method, results depend on data quality (in this case, sufficiently high-resolution data) and validity of geological model assumptions. The variability of the results obtained from onshore US magnetic data can be in part attributed to poor data coverage. For poor data coverage, low-resolution data will often result in Tilt-Depth overestimates.

Tilt-Depth is thus a new magnetic depth estimation method that lends itself to rapid mapping of sedimentary basins without the complexity of unraveling the depth solutions from methods that give multiple solutions (e.g. Euler deconvolution). Reliable depth estimates will be obtained if the inherent assumptions of the method are correct and if the magnetic data adequately sample the magnetic field. As with any magnetic depth estimation method, the Tilt-Depth methodology is more sensitive to the top surfaces of magnetic sources. This leads to potential underestimation of basin depth on the downthrown sides of fault edges. The methodology allows a rapid assessment of the subsurface geology and allows the interpreter to focus on generating a more refined basin 2D or 3D model using additional geophysical data and, where possible, constrained with seismic and well data. We wish to stress the Tilt-Depth model assumes a vertical contact extending to infinite or at least to a considerable depth extent. Vertical contacts with finite depth extent will have shallow depth estimates as found by Lee et al., 2010.

Acknowledgements

We greatly appreciate constructive and thoughtful comments of two reviewers and the Editor Dr Mark Lackie. The authors wish to thank Dr Chris Green for his help in revising the manuscript. We also acknowledge Geoscience Australia for use of the 1 km aeromagnetic dataset for Australia. We also thank Dr Swain for discussing the application of RTP to regional magnetic data.

References

Bally, A. W., 1989, Phanerozoic basins of North America, *in* A. W. Bally and A. R. Palmer, eds, The Geology of North America – an overview: Geological Society of America, pp. 397–446.

Blakely, R. J., Wells, R. E., and Weaver, C. S., 1999, Puget Sound aeromagnetic maps and data: U.S. Geological Survey Open-File Report 99–514, http://geopubs.wr.usgs.gov/open-file/of99-514, verified August 2010.

Blakely, R. J., Sherrod, B. L., Hughes, J. F., Anderson, M. L., Wells, R. E., and Weaver, C. S., 2009, Saddle Mountain fault deformation zone, Olympic Peninsula, Washington: Western boundary of the Seattle uplift: *Geosphere*, **5**, 105–125. doi:10.1130/GES00196.1

Borissova, I., and Kilgour, B., 2000, Basement Relief Image of Australian Onshore and Offshore Sedimentary Basins. Geoscience Australia GIS dataset, http://www.ga.gov.au/meta/ANZCW0703002747.html, verified August 2010.

Haddad, D., Watts, A. B., and Lindsay, J., 2001, Evolution of the intracratonic Officer Basin, central Australia: implications from subsidence analysis and gravity modeling: *Basin Research*, **13**, 217–238. doi:10.1046/j.1365-2117.2001.00147.x

Heine, C., 2007, Formation and evolution of intracontinental basins, PhD Thesis, University of Sydney.

Jachens, R. C., Griscom, A., and Roberts, C. W., 1995, Regional extent of Great Valley basement west of the Great Valley, California: implications for extensive tectonic wedging in the California Coast Ranges: *Journal of Geophysical Research*, **100**, 12 769–12 790. doi:10.1029/95JB00718

Laske, G., and Masters, S. G., 1997, A global digital map of sediment thickness: *Eos, Transactions, American Geophysical Union*, **78**, F483.

Lee, M., Morris, B., and Uglade, H., 2010, Effect of signal amplitude on magnetic depth estimations: *Leading Edge*, **29**, 672–677. doi:10.1190/1.3447778

Miller, H. G., and Singh, V., 1994, Potential field tilt – A new concept for location of potential field sources: *Journal of Applied Geophysics*, **32**, 213–217. doi:10.1016/0926-9851(94)90022-1

Milligan, P. R., Franklin, R., and Ravat, D., 2004, A new generation Magnetic Anomaly Grid Database of Australia (MAGDA): *Preview*, **113**, 25–29.

Mushayandebvu, M. F., van Driel, P., Reid, A. B., and Fairhead, J. D., 2001, Magnetic source parameters of two-dimensional structures using extended Euler deconvolution: *Geophysics*, **66**, 814–823. doi:10.1190/1.1444971

Mushayandebvu, M. F., Lesur, V., Reid, A. B., and Fairhead, J. D., 2004, Grid Euler deconvolution with constraints for 2D structures: *Geophysics*, **69**, 489–496. doi:10.1190/1.1707069

Nabighian, M.N., Grauch, V.J.S., Hansen, R.O., LaFehr, T.R., Li, Y., Peirce, J.W., Phillips, J.D., and Ruder, M.E., 2005, The historical development of the magnetic method in exploration: *Geophysics*, **70**, 33ND–61ND. doi:10.1190/1.2133784

North American Magnetic Anomaly Group, 2002, Magnetic anomaly map of North America: U.S. Geological Survey Special Map, http://pubs.usgs.gov/sm/mag_map/, verified August 2010.

Rajagopalan, S., and Milligan, P., 1994, Image enhancement of aeromagnetic data using automatic gain control: *Exploration Geophysics*, **25**, 173–178. doi:10.1071/EG994173

Ravat, D., 1996, Analysis of the Euler method and its applicability in environmental magnetic investigations: *Journal of Environmental & Engineering Geophysics*, **1**, 229–238. doi:10.4133/JEEG1.3.229

Reid, A. B., Allsop, J. M., Granser, H., Millet, A. J., and Somerton, I. W., 1990, Magnetic interpretation in three dimensions using Euler deconvolution: *Geophysics*, **55**, 80–91. doi:10.1190/1.1442774

Salem, A., and Ravat, D., 2003, A combined analytic signal and Euler method (AN-EUL) for automatic interpretation of magnetic data: *Geophysics*, **68**, 1952–1961. doi:10.1190/1.1635049

Salem, A., Williams, S., Fairhead, J. D., Ravat, D., and Smith, R., 2007, Tilt-Depth method: A simple depth estimation method using first-order magnetic derivatives: *Leading Edge*, **26**, 1502–1505. doi:10.1190/1.2821934

Snavely, P. D. Jr, and Wagner, H. C., 1963, Tertiary geologic history of western Oregon and Washington: Report of Investigation 22: Washington Division of Mines and Geology.

Swain, C. J., 2000, Reduction-to-the-pole of regional magnetic data with variable field direction, and its stabilisation at low inclinations: *Exploration Geophysics*, **31**, 78–83. doi:10.1071/EG00078

Tabor, R. W., and Cady, W. M., 1978, The structure of the Olympic Mountains, Washington – analysis of a subduction zone: Professional Paper 1033: U.S. Geological Survey.

Thomas, W. A., 1991, The Appalachian-Ouachita rifted margin of southeastern North America: *Geological Society of America Bulletin*, **103**, 415–431. doi:10.1130/0016-7606(1991)103<0415:TAORMO>2.3.CO;2

Thompson, D. T., 1982, EULDPH: A new technique for making computer-assisted depth estimates from magnetic data: *Geophysics*, **47**, 31–37. doi:10.1190/1.1441278

Thurston, J. B., and Smith, R. S., 1997, Automatic conversion of magnetic data to depth, dip, susceptibility contrast using the SPI™ method: *Geophysics*, **62**, 807–813. doi:10.1190/1.1444190

Vacquier, V., Steenland, N. C., Henderson, R. G., and Zietz, I., 1951, Interpretation of Aeromagnetic Maps: *Geological Society of America, Memoir* **47**.

Verduzco, B., Fairhead, J. D., Green, C. M., and MacKenzie, C., 2004, New insights into magnetic derivatives for structural mapping: *Leading Edge*, **23**, 116–119. doi:10.1190/1.1651454

Wells, R. E., Weaver, C. S., and Blakely, R. J., 1998, Fore-arc migration in Cascadia and its neotectonic significance: *Geology*, **26**, 759–762. doi:10.1130/0091-7613(1998)026<0759:FAMICA>2.3.CO;2

Williams, S., Fairhead, J. D., and Flanagan, G., 2005, Comparison of grid Euler deconvolution with and without 2D constraints using realistic magnetic basement models: *Geophysics*, **70**, L13–L21. doi:10.1190/1.1925745

Manuscript received 12 February 2010; accepted 17 August 2010.